Bioorganic & Medicinal Chemistry Letters 27 (2017) 2139–2143

Contents lists available at ScienceDirect

Bioorganic & Medicinal Chemistry Letters

journal homepage: www.elsevier.com/locate/bmcl

Novel scaffold evolution through combinatorial 3D-QSAR model studies of two types of JNK3 inhibitors

Hoyong Jung [a], Waqar Aman [a,b], Jung-Mi Hah [a,*]

[a] Department of Pharmacy, College of Pharmacy & Institute of Pharmaceutical Science and Technology, Hanyang University, 55 Hanyangdaehak-ro, Sangnok-gu, Ansan, Gyeonggi-do 426-791, Republic of Korea
[b] Kohat University of Science & Technology, Kohat, Khyber Pukhtunkhwa, Pakistan

ARTICLE INFO

Article history:
Received 6 February 2017
Revised 9 March 2017
Accepted 22 March 2017
Available online 24 March 2017

Keywords:
JNK3
3D-QSAR
Neurodegenerative disease

ABSTRACT

JNK3 is an emerging target for neurodegenerative diseases including AD and PD, with histological selectivity. Specifically, in AD, JNK3 is the main protein kinase for APP phosphorylation, which is an important mechanism for Aβ processing, and a biomarker of Alzheimer's disease. Therefore, targeting JNK3 is a reasonable strategy for drug discovery in neurodegenerative diseases. In order to find a novel scaffold for JNK3 inhibitors, we performed 3D-QSAR modeling studies with two different JNK3 inhibitor series. The CoMFA model was obtained with a q^2 value of 0.806 and an r^2 value of 0.850. Based on CoMFA and CoMSIA models, rational design was conducted and led to a novel scaffold, *N*-(thiophen-2-yl)-8*H*-pyrazolo[1,5-*a*]pyrido[1,2-*c*]pyrimidine-10-carboxamide.

c-Jun N-terminal kinases (JNKs) play a key role in the stress-signaling pathway involving gene expression, apoptosis, and neuronal plasticity[1] at the terminus of the MAPK pathway. Activation of JNKs through phosphorylation leads to caspase activation, neuronal inflammation, dysregulation of the cell cycle, apoptosis, and Aβ aggregation,[2] depending on the isoform. Different from JNK1 and JNK2, which are expressed throughout the body, JNK3 is mainly expressed in the brain, with small amounts expressed in the heart and testis.[3] JNK3 is an emerging target for neurodegenerative diseases, especially Alzheimer's disease (AD), because of its significant involvement in Aβ pathology.[4] First, JNK3 promotes the production of Aβ through phosphorylation of amyloid precursor protein (APP), a critical step in the process of Aβ formation and aggregation. Secondly, it is known that produced Aβ plaque uses JNK3 activation to causes neuronal toxicity, forming a positive amplifying loop in AD. Elimination of *jnk3* in FAD (familial Alzheimer's disease) mice significantly reduces Aβ 42 level and overall plaque load, increases the number of nerve cells, and improves awareness. This scheme characterizes AD as a metabolic disorder under strict control by JNK3.[5]

The JNK cascade is now understood to be an axis of molecular development for AD and other neurodegenerative pathologies; therefore, progress in the design of selective kinase inhibitors versus selective JNK inhibitors has been achieved over the years. However, identification of new compounds with increased specificity for JNK inhibition remains an open challenge.

In general, SAR (Structure-Activity Relationships) can be derived from intensive synthesis of chemical compounds and biological assays that require much effort and time. Computational approaches can predict SAR as a quantitative structure-activity relationship (QSAR) through statistical evidence with reduced physical effort. From QSAR results, compound modification that meets steric and electrostatic criteria can be proposed. Furthermore, screening a commercial chemical database larger than an in-house library generates plausible compounds worth synthesis. QSAR studies, utilizing Comparative Molecular Field Analysis (CoMFA) and Comparative Molecular Similarity Indices analysis (CoMSIA), are generally performed with a single compound series due to alignment issues. In this study, 3D-QSAR methods including comparative molecular field analysis (CoMFA) were performed to explain the activities of two different JNK3 inhibitor series known from the literature, and the results were combined into one Comparative Molecular Field Analysis (CoMFA) and Comparative Molecular Similarity Indices analysis (CoMSIA) for development of a novel scaffold for JNK3 inhibitors.

Materials and computational methods

Data set

Sets of 46 aminophenylacetamide derivatives[6] and 31 thiophen-2-yl acetamide derivatives[7] were obtained from published

* Corresponding author.
E-mail address: jhah@hanyang.ac.kr (J.-M. Hah).

http://dx.doi.org/10.1016/j.bmcl.2017.03.063
0960-894X/

literature. Of these, 9 compounds with low activity (IC_{50} > 20 μM) and 5 compounds inadequate for the CoMFA model were excluded from the 2-aminophenylacetamide derivatives. In total, 63 compounds were selected for the QSAR model. The pIC_{50} values were used as a dependent variable in the QSAR model. The 63 compounds were divided into a training set of 50 compounds to generate a QSAR model and a test set of 13 compounds. The compound series are listed in Tables 1 and 2.

Preparation of ligands and receptor

Complex structures of JNK3 with inhibitors **7** and **34** were obtained from the PDB (code: 3FV8, 3RTP) and were used in the Protein Preparation Wizard of the Schrödinger Maestro program.[8] All water molecules and debris were removed from the structures. The structures of other compounds were prepared on the basis of the conformations of **7** and **34**, and their 3D conformations were generated using the SYBYL-X Ligand Preparation; Quick 3D.[9]

Alignments for CoMFA and CoMSIA

In order to mimic the bioactive conformation, all compounds were docked with each protein prepared previously using Schrödinger Grid generation and Ligand docking. For comparison of protein-ligand complexes, 3D conformations of compounds were generated and trimmed manually for alignment. The furan and thiophene moieties and amide and reverse amide bonds were fit, respectively, to align the different compound series. Next, the benzylpiperazine and fused 6-membered ring moieties were aligned in bioactive conformations (Fig. 2). Finally, all compounds were aligned using SYBYL-X Distill Rigid (Fig. 1).[10]

CoMFA

The pIC_{50} values of training sets containing the two series and CoMFA as a descriptor were used for a CoMFA model. Descriptors were processed with Gasteiger-Hückel atomic charges. Next, CoMFA modeling was conducted using SYBYL-X 2.1.1 automatic PLS.[11] The statistical parameters of the CoMFA model are listed in Table 3.

CoMSIA

A similar process was conducted for the CoMSIA model. As descriptors, steric, electrostatic, hydrophobic, hydrogen bond donor, and hydrogen bond acceptor indices were selected. The statistical parameters of the CoMSIA model are listed in Table 3.

Results and discussions

CoMFA and COMSIA contour maps

Steric and electrostatic contour maps are shown in Figs. 3 and 4. In the contour maps, the steric field was visualized as a green region that favors bulkiness and a yellow region that disfavors bulkiness. As shown in Fig. 3, the heteroaromatic ring substituted

Table 1
Structures of 2-aminophenylacetamide derivatives and their JNK3 inhibitory activities.

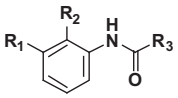

No.	Substituents			Activity (μM)	
	R^1	R^2	R^3	IC_{50}	pIC_{50}
1	Cl	4-Ethyl-1-piperazinyl	2-Bromo-5-furanyl	1.1	5.959
2	Cl	4-Methyl-1-piperazinyl	2-Bromo-5-furanyl	1.2	1.200
3	Cl	4-*n*-Propyl-1-piperazinyl	2-Bromo-5-furanyl	0.9	0.900
4	Cl	4-*i*-Propyl-1-piperazinyl	2-Bromo-5-furanyl	2.2	5.658
5	Cl	4-Allyl-1-piperazinyl	2-Bromo-5-furanyl	0.33	6.481
6	Cl	4-(3-Methylbut-3-en-1-yl)-1-piperazinyl	2-Bromo-5-furanyl	0.54	6.268
7	Cl	4-(Prop-2-yn-1-yl)-1-piperazinyl	2-Bromo-5-furanyl	0.16	6.796
8	Cl	4-Cyclopropyl-1-piperazinyl	2-Bromo-5-furanyl	0.96	6.018
9	Cl	4-(Furan-2-ylmethyl)-1-piperazinyl	2-Bromo-5-furanyl	0.25	6.602
10	Cl	4-Phenylmethyl-1-piperazinyl	2-Bromo-5-furanyl	1.1	5.959
11	Cl	4-(2-Phenylethane-1-yl) -1-piperazinyl	2-Bromo-5-furanyl	1.4	5.854
12	Cl	4-(2-Pyridyl)-1-piperazinyl	2-Bromo-5-furanyl	1.0	1.000
13	Cl	4-(2-Oxopropan-1-yl) -1-piperazinyl	2-Bromo-5-furanyl	0.81	6.092
14	Me	4-Allyl-1-piperazinyl	2-Bromo-5-furanyl	0.20	6.699
15	F	4-(Prop-2-yn-1-yl)-1-piperazinyl	2-Bromo-5-furanyl	0.29	6.538
16	Cl	4-Allyl-1-piperazinyl	4-Bromothiazol-3-yl	1.8	5.745
17	Cl	4-Allyl-1-piperazinyl	Thiazol-4-yl	2.3	5.638
18	Cl	4-Allyl-1-piperazinyl	Isoxazol-5-yl	5.0	5.301
19	Cl	4-Allyl-1-piperazinyl	2-Pyrrolyl	8.9	5.051
20	Cl	4-Allyl-1-piperazinyl	2-Methylthiazol-4-yl	5.8	5.237
21	Cl	4-Allyl-1-piperazinyl	2-Bromopyridin-6-yl	2.0	5.699
22	Cl	4-Allyl-1-piperazinyl	2-Methylpyridin-6-yl	2.0	5.699
23	Cl	4-Allyl-1-piperazinyl	Bromobenzen-3-yl	6.4	5.194
24	Me	1,4-Dioxa-8-azaspiro[4.5]decan-8-yl	2-Bromo-5-furanyl	0.06	7.222
25	Me	1,4-Dioxa-8-azaspiro[4.5]decan-8-yl	2-Chloro-5-furanyl	0.08	7.097
26	Me	1,4-Dioxa-8-azaspiro[4.5]decan-8-yl	2-Fluoro-5-furanyl	0.41	6.387
27	Me	1,4-Dioxa-8-azaspiro[4.5]decan-8-yl	2-Cyano-5-furanyl	0.21	6.678
28	Me	1,4-Dioxa-8-azaspiro[4.5]decan-8-yl	5-Methyl-2-furanyl	0.53	6.276
29	Me	1,4-Dioxa-8-azaspiro[4.5]decan-8-yl	2-(Fluoromethyl)furan-5-yl	0.35	6.456
30	Me	1,4-Dioxa-8-azaspiro[4.5]decan-8-yl	2-Ethylfuran-5-yl	0.10	7.000
31	Me	1,4-Dioxa-8-azaspiro[4.5]decan-8-yl	2-(Prop-2-yn-1-yl)furan-5-yl	0.11	6.959
32	Me	1,4-Dioxa-8-azaspiro[4.5]decan-8-yl	2-Methoxyfuran5-yl	0.62	6.208